Pergamon

Int. J. Heat Mass Transfer. Vol. 39, No. 3, pp. 615–630, 1996

0017-9310/96 $9.50+0.00

0017-9310(95)00155-7

Buoyancy-induced flow adjacent to a periodically heated and cooled horizontal surface in porous media

R. BRADEAN† and D. B. INGHAM
Department of Applied Mathematical Studies, The University of Leeds, Leeds LS2 9JT, U.K.

P. J. HEGGS
Department of Chemical Engineering UMIST, Manchester M60 1QD, U.K.

and

I. POP
Faculty of Mathematics, The University of Cluj, R-3400 Cluj, CP 253, Romania

(*Received* 8 *January* 1995)

Abstract—Analytical and numerical solutions are presented for the problem of steady, natural convection from a sinusoidally heated and cooled horizontal surface which is embedded in a fluid saturated porous media which is maintained at a constant temperature T_∞. The plate is assumed to have a harmonic temperature variation, and at large distances from the plate we investigate two different boundary conditions, namely, when we enforce either a constant temperature T_∞ or an adiabatic boundary condition. For small values of the Rayleigh number an analytical solution has been obtained provided that the temperature at infinity is constant but depends on the Rayleigh number or there is zero heat flux at infinity. On specifying an arbitrary temperature T_∞ at infinity then no analytical solution could be obtained and the numerical solution procedure was not convergent. However, we were able to obtain an analytical solution in the situation when the constant temperature T_∞ is enforced at a finite distance, say $y = d$, from the plate and, as $d \to \infty$, the solution approaches that obtained by enforcing the adiabatic condition at infinity. When the constant temperature T_∞ is enforced at the station $y = d$ we found that the numerical solution is dependent on the value of d, but when the zero heat flux condition is enforced at $y = d$ we obtained that $d = 4\pi$ is sufficiently large for the solution to be independent of the value of d. At very small values of Ra there is very good agreement between the analytical and numerical solutions and when Ra is very large the boundary-layer scalings for the Nusselt number and the mean fluid velocity along the plate are confirmed by the numerical calculations.

1. INTRODUCTION

Theoretical and experimental research on the mechanism of convective heat transfer in porous media has been well established for many practical applications, such as geothermal reservoirs, insulation of buildings and equipment, storage of radioactive nuclear waste materials, engineering aspects of irrigation systems, separation processes in chemical industries and oil recovery techniques to name but a few. A very good and comprehensive review of the state of knowledge of convective heat transfer mechanism through porous media has recently been given by Nield and Bejan [1]. Most of these studies consider two kinds of boundary conditions, namely, when the surface temperature or the heat flux from the surface are simple power functions of the distance measured from the leading edge of a plane vertical or horizontal surface which is embedded in a porous media. Cheng and Minkowycz [2] analysed the steady-state case of a vertical wall at very large values of the Rayleigh number. Using the boundary-layer approximations, the governing partial, non-linear differential equations were transformed into a set of coupled ordinary differential equations which were integrated numerically using the Runge–Kutta method. Similarity solutions were also obtained by Cheng and Chang [3] for the free convection fluid flow in a saturated porous media above a heated horizontal impermeable surface. The reverse situation, namely that of natural convection from a cooled plate facing upwards was analysed by Kimura *et al.* [4] by using a scale analysis and the Karman–Pohlhausen integral method. Finite-difference solutions were also obtained for Rayleigh numbers as large as 700. Merkin and Zhang [5] considered the free convection fluid flow in an infinite horizontal porous channel with the bottom wall being partially heated

† On leave from Faculty of Mathematics, The University of Cluj, R-3400 Cluj, CP 253, Romania.

NOMENCLATURE

c	constant, equation (49)
d	non-dimensional distance from the plate
D	solution domain
g	acceleration due to gravity
H	non-dimensional height of the cells formed along the heated and cooled horizontal surface
K	permeability of the porous media
L	a characteristic length
$m+1$	number of nodal poins in the x direction
$n+1$	number of nodal points in the y direction
Nu	Nusselt number
$p+1$	number of nodal points in the z direction
Q	heat flux
Ra	Rayleigh number
T	non-dimensional temperature
T_a	temperature
u, v	non-dimensional velocity components along x and y directions, respectively
U_c	a characteristic velocity
x, y	non-dimensional Cartesian coordinates along and normal to the plate, respectively
z	transformed coordinate, equation (51).

Greek symbols

α	thermal diffusivity
β	coefficient of thermal expansion
ν	kinematic viscosity of the convective fluid
ψ	non-dimensional streamfunction
ε	convergence parameter, equation (59).

Superscripts

$\hat{}$	dimensional variables
$\bar{}$	average quantities
$\tilde{}$	boundary-layer variables
s	order of iterations.

Subscripts

i, j	nodal points
inf	value at infinity
∞	condition at infinity.

or cooled. For the heated case and at a certain value of the aspect ratio of the channel, they found a range of values of the Rayleigh number over which two different finite-difference solutions exist.

However, there has been very little work performed on convective flows from surfaces immersed in a porous media which are subject to other types of temperature boundary conditions. In this paper, we consider the steady, free convection flow induced by a harmonically (cosine function) heated and cooled infinite horizontal surface that delimits a semi-infinite porous media. The first paper to deal with this flow and heat transfer configuration was undertaken by Poulikakos and Bejan [6], who assumed that the porous media is maintained at a constant temperature T_0 at very large distances from the plate and that the wall temperature distribution is of the form

$$\hat{T} = T_a \cos(\hat{x}/L) + T_0 \tag{1}$$

where T_a is the amplitude of the wall temperature variations, $2\pi L$ is the period of the length scale oscillations and $\hat{x}$ is the distance along the plate. This problem was studied from a finite penetration point of view, namely it was assumed that only a finite region of the porous media is affected by the spatial periodic temperature variations along the plate. Therefore, the boundary condition $T = T_0$ was imposed at a very large distance from the plate which increases as the Rayleigh number increases. Finite difference solutions were obtained and a scale analysis was performed to show that the natural circulation consists of a row of counter-rotating cells situated close to the horizontal surface. It was found that the cellular flow penetrates into the porous media vertically to a distance of approximately $LRa^{1/2}$, where Ra is the Rayleigh number. The effects of heated and cooled walls in porous media were also investigated by Poulikakos and Bejan [7], who described the free convection flow in a porous media enclosed by a rectangular domain having a temperature distribution on one vertical side of the step function form, the other three boundaries being insulated. A scale analysis and a finite-difference method were employed in two situations, namely, when the side heating effect is positioned above and below the side cooling effect. In this paper we consider the same problem considered by Poulikakos and Bejan [6], i.e. with the horizontal wall temperature distribution of the form (1), but at very large distances from the plate, $\hat{y} \to \infty$, we analyse two situations, namely, when a given temperature T_∞ or an adiabatic boundary condition is enforced. We first present analytical solutions for the governing equations using a series expansion method in terms of small Rayleigh number, Ra. When the temperature on the plate is specified by the cosine function, we found that the temperature at infinity is a non-zero constant and its value depends on the value of Ra. This analytical solution is physically consistent with having an average zero heat flux both at $\hat{y} = 0$ and at infinity. In order to investigate how the solution with an infinite domain is approached from the situation when there is a boundary condition at a large but finite distance

from the plate, an analytical solution of the governing equations has been also obtained when a prescribed constant temperature boundary condition is enforced at a finite distance from the plate $\hat{y} = d$. From this solution it is easily seen that as $d \to \infty$, the small Rayleigh number solution becomes identical to the solution obtained by enforcing $\partial\hat{T}/\partial\hat{y} \to 0$ as $\hat{y} \to \infty$. Therefore, it is concluded that the boundary condition of no heat transfer at an infinite distance from the plate is the appropriate physical boundary condition to enforce. Poulikakos and Bejan [6] have not considered the adiabatic boundary condition at infinity, and specifying the temperature at infinity proves to be an erroneous interpretation of penetration.

Detailed numerical solutions of the governing equations using a finite-difference method are also obtained for a large range of values of the Rayleigh number $0 \leqslant Ra \leqslant 200/\pi$. A comparison of the analytical and numerical solutions of the streamline and isotherm patterns, the mean fluid velocity along the plate, the mean Nusselt number, the average heat flux at the plate and the temperature at an infinite distance from the plate show excellent agreement at small values of the Rayleigh number.

2. GOVERNING EQUATIONS

We consider an infinite horizontal surface which is embedded in a homogeneous fluid-saturated porous media of ambient temperature T_∞. It is assumed that the temperature of the surface varies harmonically about the mean value of T_0, as given by equation (1) and a Cartesian system of coordinates with the $\hat{x}$ and $\hat{y}$ axes taken along and normal to the surface, respectively, has been chosen. At large distances from the plate we consider two different physical boundary conditions, namely, either a constant temperature T_∞ or zero heat flux is enforced, i.e.

$$\hat{T} \to T_\infty \quad \text{as} \quad \hat{y} \to \infty \quad -\infty < \hat{x} < \infty \tag{2}$$

or

$$\partial\hat{T}/\partial\hat{y} \to 0 \quad \text{as} \quad \hat{y} \to \infty \quad -\infty < \hat{x} < \infty. \tag{3}$$

The fluid velocity and the pores of the porous media are assumed to be small so that Darcy's model is valid. Under these assumptions and the application of the Boussinesq approximation, the governing equations can be written in non-dimensional form, see Nield and Bejan [1], as

$$\frac{\partial^2\psi}{\partial x^2} + \frac{\partial^2\psi}{\partial y^2} = -\frac{\partial T}{\partial x} \tag{4}$$

$$\frac{\partial^2 T}{\partial x^2} + \frac{\partial^2 T}{\partial y^2} = Ra\left(\frac{\partial\psi}{\partial y}\frac{\partial T}{\partial x} - \frac{\partial\psi}{\partial x}\frac{\partial T}{\partial y}\right) \tag{5}$$

where $Ra = gK\beta T_a L/\alpha\nu$ is the Rayleigh number, ψ is the streamfunction defined in the usual way, namely $u = \partial\psi/\partial y$ and $v = -\partial\psi/\partial x$, and the non-dimensional variables are defined in the form

$$x = \hat{x}/L \quad y = \hat{y}/L \quad \psi = \hat{\psi}/(U_c L) \quad T = (\hat{T} - T_0)/T_a \tag{6}$$

where $U_c = gK\beta T_a/\nu$ is a characteristic velocity. Since the problem is periodic in the x direction, we need only solve equations (4) and (5) in the domain

$$D = \{(x, y) \in E^2 : 0 \leqslant x \leqslant 2\pi, 0 \leqslant y < \infty\} \tag{7}$$

and we have

$$\psi(0, y) = \psi(2\pi, y) \quad T(0, y) = T(2\pi, y) \tag{8}$$

for all values of $y \in [0, \infty)$. It can be easily shown that the temperature and the streamfunction are symmetrical about the plane $x = \pi$, i.e. $T(x, y) = T(2\pi - x, y)$ and $\psi(x, y) = -\psi(2\pi - x, y)$ where $0 \leqslant x \leqslant \pi$ and $0 \leqslant y < \infty$. Thus, the problem reduces to solving equations (4) and (5) in the domain

$$D_0 = \{(x, y) \in E^2 : 0 \leqslant x \leqslant \pi, 0 \leqslant y < \infty\} \tag{9}$$

subject to the following boundary conditions

$$\psi = 0 \quad T = \cos(x) \quad y = 0 \quad 0 \leqslant x \leqslant \pi \tag{10}$$

$$\psi = 0 \quad \partial T/\partial x = 0 \quad x = 0, \pi \quad 0 \leqslant y < \infty \tag{11}$$

and either

$$\psi \to 0 \quad T \to \frac{T_\infty - T_0}{T_a} \quad y \to \infty \quad 0 \leqslant x \leqslant \pi \tag{12}$$

or

$$\psi \to 0 \quad \partial T/\partial y \to 0 \quad y \to \infty \quad 0 \leqslant x \leqslant \pi. \tag{13}$$

Further, we will initially seek solutions such that $T_\infty = T_0$.

3. ANALYTICAL SOLUTION FOR SMALL VALUES OF THE RAYLEIGH NUMBER

A regular perturbation method is employed to obtain approximate solutions of equations (4) and (5) subject to the boundary conditions (10)–(13), i.e. we look for solutions of these equations of the form

$$\psi = \psi_0(x, y) + (Ra)\psi_1(x, y) + (Ra^2)\psi_2(x, y) + \mathbf{0}(Ra^3) \tag{14}$$

$$T = T_0(x, y) + (Ra)T_1(x, y) + (Ra^2)T_2(x, y) + \mathbf{0}(Ra^3). \tag{15}$$

By substituting expressions (14) and (15) into equations (4) and (5), and equating the same powers of Ra, we obtain the following partial differential equations

$$\frac{\partial^2 T_0}{\partial x^2} + \frac{\partial^2 T_0}{\partial y^2} = 0 \tag{16}$$

$$\frac{\partial^2\psi_0}{\partial x^2} + \frac{\partial^2\psi_0}{\partial y^2} = -\frac{\partial T_0}{\partial x} \tag{17}$$

$$\frac{\partial^2 T_1}{\partial x^2}+\frac{\partial^2 T_1}{\partial y^2}=\frac{\partial \psi_0}{\partial y}\frac{\partial T_0}{\partial x}-\frac{\partial \psi_0}{\partial x}\frac{\partial T_0}{\partial y} \quad (18)$$

$$\frac{\partial^2 \psi_1}{\partial x^2}+\frac{\partial^2 \psi_1}{\partial y^2}=-\frac{\partial T_1}{\partial x} \quad (19)$$

$$\frac{\partial^2 T_2}{\partial x^2}+\frac{\partial^2 T_2}{\partial y^2}=\frac{\partial \psi_0}{\partial y}\frac{\partial T_1}{\partial x}-\frac{\partial \psi_0}{\partial x}\frac{\partial T_1}{\partial y}+\frac{\partial \psi_1}{\partial y}\frac{\partial T_0}{\partial x}-\frac{\partial \psi_1}{\partial x}\frac{\partial T_0}{\partial y} \quad (20)$$

$$\frac{\partial^2 \psi_2}{\partial x^2}+\frac{\partial^2 \psi_2}{\partial y^2}=-\frac{\partial T_2}{\partial x} \quad (21)$$

which have to be solved subject to the boundary conditions (10)–(13) which become, on using of expressions (14) and (15),

$$\psi_0=0 \quad T_0=\cos(x) \quad y=0 \quad 0\leqslant x\leqslant \pi \quad (22)$$

$$\psi_k=0 \quad T_k=0 \quad k=1,2,\ldots y=0 \quad 0\leqslant x\leqslant \pi \quad (23)$$

$$\psi_k=0 \quad \partial T_k/\partial x=0 \quad k=0,1,\ldots \quad x=0,\pi \quad 0\leqslant y<\infty \quad (24)$$

and either

$$\psi_k\to 0 \quad T_k\to 0 \quad k=0,1,\ldots \quad y\to\infty \quad 0\leqslant x\leqslant\pi \quad (25)$$

or

$$\psi_k\to 0 \quad \partial T_k/\partial y\to 0 \quad k=0,1,\ldots \quad y\to\infty \quad 0\leqslant x\leqslant\pi. \quad (26)$$

We first consider the situation in which the boundary condition (25) is enforced at infinity. Solving equations (16) and (17) we obtain

$$T_0=e^{-y}\cos(x) \quad (27)$$

$$\psi_0=-\tfrac{1}{2}y e^{-y}\sin(x) \quad (28)$$

which on substitution into equation (18) gives

$$\frac{\partial^2 T_1}{\partial x^2}+\frac{\partial^2 T_1}{\partial y^2}=\tfrac{1}{4}(1-2y)e^{-2y}-\tfrac{1}{4}e^{-2y}\cos(2x). \quad (29)$$

However, on solving this equation, we are unable to obtain a solution which satisfies both boundary conditions (22) and (25) for T_1, and the only solution which satisfies the boundary condition (22) is found to be

$$T_1=-\tfrac{1}{16}(1+2y)e^{-2y}+\tfrac{1}{16}y e^{-2y}\cos(2x)+\tfrac{1}{16}. \quad (30)$$

This solution does not satisfy the boundary condition at infinity (25), since $T_1\to 1/16$ as $y\to\infty$. A singular perturbation method was sought but we were unable to match the inner and outer solutions. However, it should be observed that the functions T_0, ψ_0 and T_1 satisfy the boundary condition (26) as $y\to\infty$. Therefore, we shall obtain higher-order approximations for the streamfunction and temperature in the regular perturbation method but using the boundary condition (26) at infinity. The solutions of equations (19)–(21) are found to be given by

$$\psi_1=-\tfrac{1}{64}(\tfrac{1}{2}y+y^2)e^{-2y}\sin(2x) \quad (31)$$

$$T_2=\tfrac{1}{256}[-\tfrac{3}{8}e^{-y}+(\tfrac{3}{8}-y^2)e^{-3y}]\cos(x)+\tfrac{1}{384}(\tfrac{7}{12}y+y^2)e^{-3y}\cos(3x) \quad (32)$$

$$\psi_2=\tfrac{1}{2048}[(\tfrac{1}{2}+\tfrac{3}{2}y)e^{-y}-(\tfrac{1}{2}+\tfrac{3}{2}y+y^2)e^{-3y}]\sin(x)-\tfrac{1}{4608}(\tfrac{11}{12}y+\tfrac{11}{4}y^2+2y^3)e^{-3y}\sin(3x). \quad (33)$$

Further terms in the expansion equations (14) and (15) have been found but the lengths of these expressions become excessively large and therefore are not presented here. From this solution, analytical expressions for the mean velocity along the plate $\bar{u}$, the mean Nusselt number $\overline{Nu}$, the average heat flux at the plate $\bar{Q}$ and the temperature at infinity T_{inf} are obtained in the form

$$\bar{u}=\int_0^{\pi}u(x,0)\,dx=-1+\tfrac{35}{41472}Ra^2+\mathbf{0}(Ra^3) \quad (34)$$

$$\overline{Nu}=\int_0^{\pi/2}\left(-\frac{\partial T}{\partial y}\right)_{y=0}dx=1+\tfrac{95}{27648}Ra^2+\mathbf{0}(Ra^3) \quad (35)$$

$$\bar{Q}=\int_0^{\pi}\left(\frac{\partial T}{\partial y}\right)_{y=0}dx=\mathbf{0}(Ra^4) \quad (36)$$

$$T_{\text{inf}}=\tfrac{1}{16}Ra-\tfrac{19}{131072}Ra^3+\mathbf{0}(Ra^4). \quad (37)$$

We now consider the situation in which the boundary condition (25) is enforced at a finite distance, namely $y=d$, rather than at infinity. The problem now reduces to solving equations (16)–(21) subject to the boundary conditions (22) and

$$\psi_k=0 \quad \partial T_k/\partial x=0 \quad k=0,1,\ldots \quad x=0,\pi \quad 0\leqslant y<d \quad (38)$$

$$\psi_k=0 \quad T_k=0 \quad k=0,1,\ldots \quad y=d \quad 0\leqslant x\leqslant\pi \quad (39)$$

and we obtain

$$T_0=\frac{1}{2(1-e^{-2d})}(e^{-y}-e^{y-2d})\cos(x) \quad (40)$$

$$\psi_0=-\frac{y}{2(1-e^{-2d})}(e^{-y}-e^{y-2d})\sin(x) \quad (41)$$

$$T_1 = \frac{1}{4(1-e^{-2d})^2}\left\{-(\tfrac{1}{4}+\tfrac{1}{2}y)\,e^{-2y}+(-\tfrac{1}{4}+\tfrac{1}{2}y)\,e^{2y-4d}\right.$$
$$-y^2 e^{-2d}+\left[-\frac{1}{4d}+\left(\frac{1}{2d}+d\right)e^{-2d}-\frac{1}{4d}e^{-4d}\right]y$$
$$+\tfrac{1}{4}e^{-4d}+\tfrac{1}{4}+\tfrac{1}{2}\left(\frac{1}{1+e^{2d}}+\tfrac{1}{2}y\right)e^{-2y}\cos(2x)$$
$$\left.+\frac{1}{2}\left(\frac{e^{2d}}{1+e^{2d}}-\tfrac{1}{2}y\right)e^{2y-4d}\cos(2x)-\tfrac{1}{4}e^{-2d}\cos(2x)\right\} \tag{42}$$

$$\psi_1 = \frac{1}{16(1-e^{-2d})^2}\left\{-\frac{1}{1+e^{2d}}y\,e^{-2y}\right.$$
$$+\frac{1}{1+e^{-2d}}y\,e^{2y-4d}+\tfrac{1}{2}e^{-2d}-(\tfrac{1}{8}y+\tfrac{1}{4}y^2)\,e^{-2y}$$
$$+(\tfrac{1}{8}y-\tfrac{1}{4}y^2)\,e^{2y-4d}+\left[\frac{d}{(1+e^{2d})^2}\right.$$
$$\left.+\frac{(1-d^2)\,e^{-2d}-1}{2(e^{2d}-e^{-2d})}\right]e^{-2y}-\left[\frac{d}{(1+e^{2d})^2}\right.$$
$$\left.\left.+\frac{(1-d^2)\,e^{-2d}-e^{-4d}}{2(e^{2d}-e^{-2d})}\right]e^{2y}\right\}\sin(2x). \tag{43}$$

Using expressions (40)–(43), the mean velocity along the plate, the mean Nusselt number and the average heat flux at $y = 0$ are found to be given by

$$\bar{u} = -1+\mathbf{0}(Ra^2) \tag{44}$$

$$\overline{Nu} = \frac{1}{1-e^{-2d}}+\frac{\pi}{8(1-e^{-2d})^2}\left[\frac{1}{4d}-\left(\frac{1}{2d}+d\right)e^{-2d}\right.$$
$$\left.+\frac{1}{4d}e^{-4d}\right]Ra+\mathbf{0}(Ra^2) \tag{45}$$

$$\bar{Q} = -\frac{\pi}{4(1-e^{-2d})^2}\left[\frac{1}{4d}-\left(\frac{1}{2d}+d\right)e^{-2d}\right.$$
$$\left.+\frac{1}{4d}e^{-4d}\right]Ra+\mathbf{0}(Ra^2). \tag{46}$$

It is important to note that as $d\to\infty$, the second approximation for the temperature given by expression (42), which satisfies $T_1 = 0$ at $y = d$, tends to the solution of equation (29) given by expression (30), for which $T_1 = 1/16$ at infinity. In fact, in the limit $d\to\infty$, all of the expressions (40)–(46) reduce to those given by (27), (28), (30)–(37).

4. NUMERICAL SOLUTION

In order to solve numerically equations (4) and (5) along with the boundary conditions (10)–(13), we divide the solution domain D_0 into two regions, namely,

$$D_a = \{(x,y)\in E^2 : 0\leqslant x\leqslant\pi, 0\leqslant y\leqslant d\} \tag{47}$$

$$D_b = \{(x,y)\in E^2 : 0\leqslant x\leqslant\pi, d\leqslant y<\infty\} \tag{48}$$

where d is a positive constant to be specified and $D_0 = D_a\cup D_b$. By using the transformation proposed by Zeldin and Schmidt [8], namely,

$$z = 1-\frac{1}{1+c(y-d)} \tag{49}$$

where c is a parameter to be determined, the semi-infinite domain D_b is transformed into the finite domain D_c given by

$$D_c = \{(x,z)\in E^2 : 0\leqslant x\leqslant\pi, 0\leqslant z\leqslant 1\}. \tag{50}$$

Using the transformation (49), equations (4) and (5) can be transformed in the domain D_c as

$$\frac{\partial^2\psi}{\partial x^2}+c^2(1-z)^4\frac{\partial^2\psi}{\partial z^2}-2c^2(1-z)^3\frac{\partial\psi}{\partial z} = -\frac{\partial T}{\partial x} \tag{51}$$

$$\frac{\partial^2 T}{\partial x^2}+c^2(1-z)^4\frac{\partial^2 T}{\partial z^2}-2c^2(1-z)^3\frac{\partial T}{\partial z}$$
$$= Rac(1-z)^2\left(\frac{\partial\psi}{\partial z}\frac{\partial T}{\partial x}-\frac{\partial\psi}{\partial x}\frac{\partial T}{\partial z}\right) \tag{52}$$

while the boundary conditions (10)–(13) become

$$\psi(x,y) = 0 \quad T(x,y) = \cos(x) \quad y = 0 \quad 0\leqslant x\leqslant\pi \tag{53}$$

$$\psi(x,y) = 0 \quad \partial T/\partial x(x,y) = 0 \quad x = 0,\pi \quad 0\leqslant y\leqslant d \tag{54}$$

$$\psi(x,z) = 0 \quad \partial T/\partial x(x,z) = 0 \quad x = 0,\pi \quad 0\leqslant z\leqslant 1 \tag{55}$$

and either

$$\psi(x,z) = 0 \quad T(x,z) = 0 \quad z = 1 \quad 0\leqslant x\leqslant\pi \tag{56}$$

or

$$\psi(x,z) = 0 \quad \partial T/\partial z(x,z) = 0 \quad z = 1 \quad 0\leqslant x\leqslant\pi. \tag{57}$$

The problem now reduces to solving equations (4) and (5) in the domain D_a subject to the boundary conditions (53) and (54), and equations (51) and (52) in the domain D_c subject to the boundary conditions (55) and (56) or (57). The central-difference method was used to solve these equations numerically, and in order to match the grids in the domains D_a and D_c, which contain $m+1$ points in the x direction $\{x_1 = 0, x_2, \ldots, x_{m+1} = \pi\}$, $n+1$ points in the y direction $\{y_1 = 0, y_2, \ldots, y_{n+1} = d\}$ and $p+1$ points in the z direction $\{z_{n+1} = 0, z_{n+2}, \ldots, z_{n+p+1} = 1\}$, we found that

$$c = \frac{n}{d(p-1)}. \tag{58}$$

The resulting system of non-linear algebraic equations is solved using the Succesive Over Relaxation iterative method, which is terminated when

$$\Delta\psi^{(s)} = \max\{|\psi_{i,j}^{(s)} - \psi_{i,j}^{(s-1)}| : i = 1,2,\ldots,m+1, \quad j = 1,2,\ldots,n+p+1\} < \varepsilon \quad (59)$$

$$\Delta T^{(s)} = \max\{|T_{i,j}^{(s)} - T_{i,j}^{(s-1)}| : i = 1,2,\ldots,m+1, \quad j = 1,2,\ldots,n+p+1\} < \varepsilon \quad (60)$$

where the notation $(\ )_{i,j}$ means the value of the function at the grid point (x_i, y_j) or (x_i, z_j), the subscript s denotes the order of the iteration and ε is some prescribed small value, say $\varepsilon = 10^{-9}$. Numerical calculations were obtained for the Rayleigh number Ra ranging from 0 to $200/\pi$ and for the two boundary conditions at infinity as given by (12) and (13). These boundary conditions were first imposed at various finite locations $y = d$ where $3\pi \leqslant d < \infty$ and we have investigated the dependence of the solution on the value of d for different values of Ra. Then we numerically obtained results by imposing the boundary conditions (12) and (13) exactly at infinity using the transformation (49). Numerical results were obtained for two grids of step sizes $\pi/20$ and $\pi/40$ in the x and y directions, and 1/30 and 1/60 in the z direction. We found that the mean velocity along the plate and the mean Nusselt number calculated using these grids agree within 0.3% for $Ra = 1/\pi$ and 1% for $Ra = 200/\pi$ and for all locations d considered. Therefore all the results presented in this paper are for a step size of $\pi/40$ in the x and y directions and 1/60 in the z direction.

5. RESULTS AND DISCUSSION

In order to illustrate the nature of the numerical solution, the streamline and isotherm patterns are plotted in Figs. 1–7 for different values of Ra and for both boundary conditions (12) and (13) imposed either at a finite distance, $y = d$, from the plate or at infinity. Since the temperature on the plate differs from that of the surrounding fluid, i.e. T_∞, a vertical density gradient is generated in the fluid adjacent to the plate and this induces a longitudinal pressure gradient. A convective movement sets up in the fluid along the plate in the direction of decreasing pressure, i.e. increasing temperature along the plate. Therefore, streams of opposite directions develop just above the plate between cold and hot locations. Two adjacent streams meet at a hot location and give rise to an upward vertical stream, which turns to fill the vacuum created near the cold locations. Thus a row of counter rotating cells develop near the plate. Since the fluid near the hot locations rises and the fluid near the cold

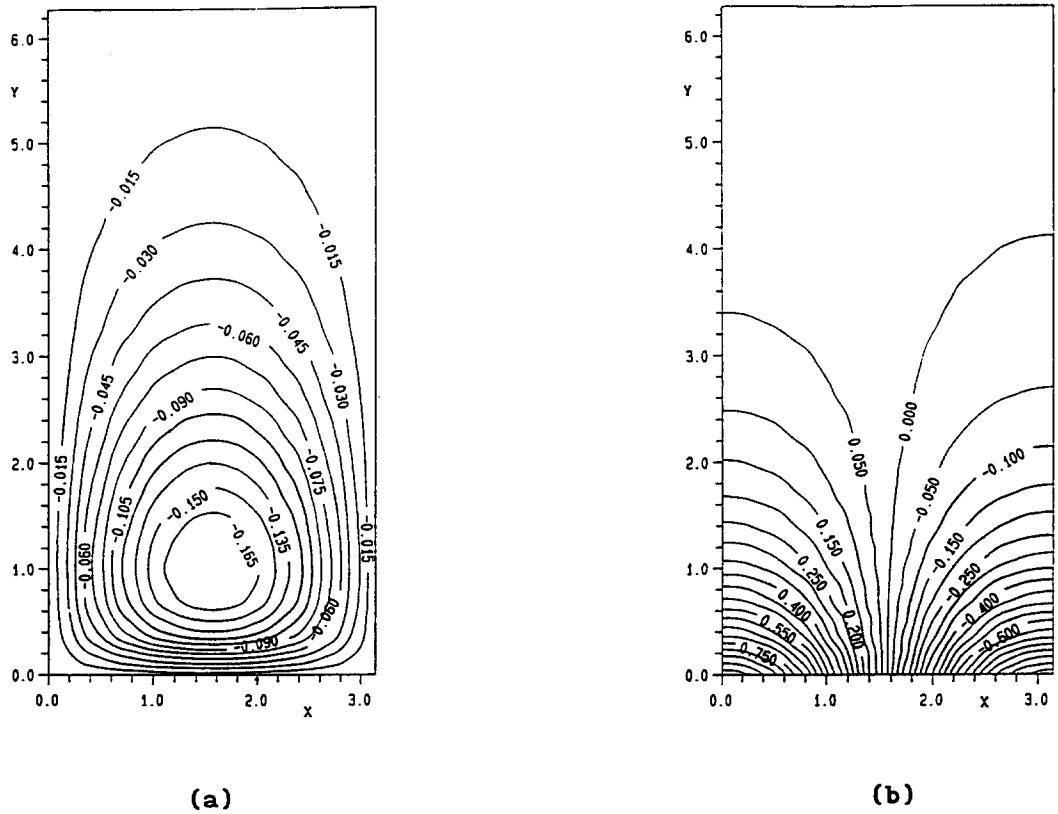

Fig. 1. Streamlines (a) and isotherms (b) for $Ra = 1/\pi$ plotted in the region $\{0 \leqslant x \leqslant \pi, 0 \leqslant y \leqslant 2\pi\}$ using the fixed temperature boundary condition (12) at $y = d = 7\pi$.

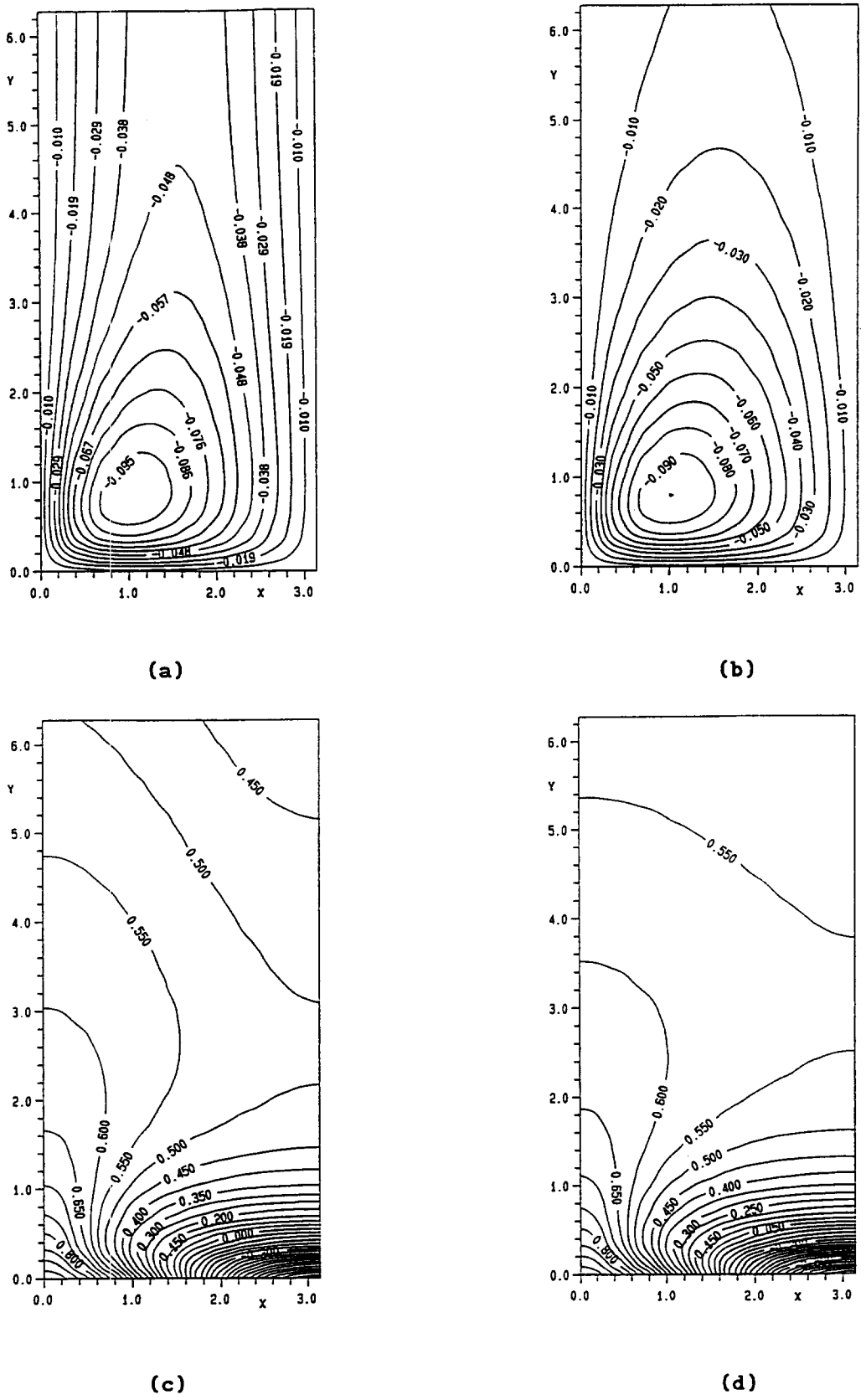

Fig. 2. Streamlines (a), (b) and isotherms (c), (d) for $Ra = 100/\pi$ plotted in the region $\{0 \leqslant x \leqslant \pi, 0 \leqslant y \leqslant 2\pi\}$ using the fixed temperature boundary condition (12) at $y = d = 6\pi$ and 8π, respectively.

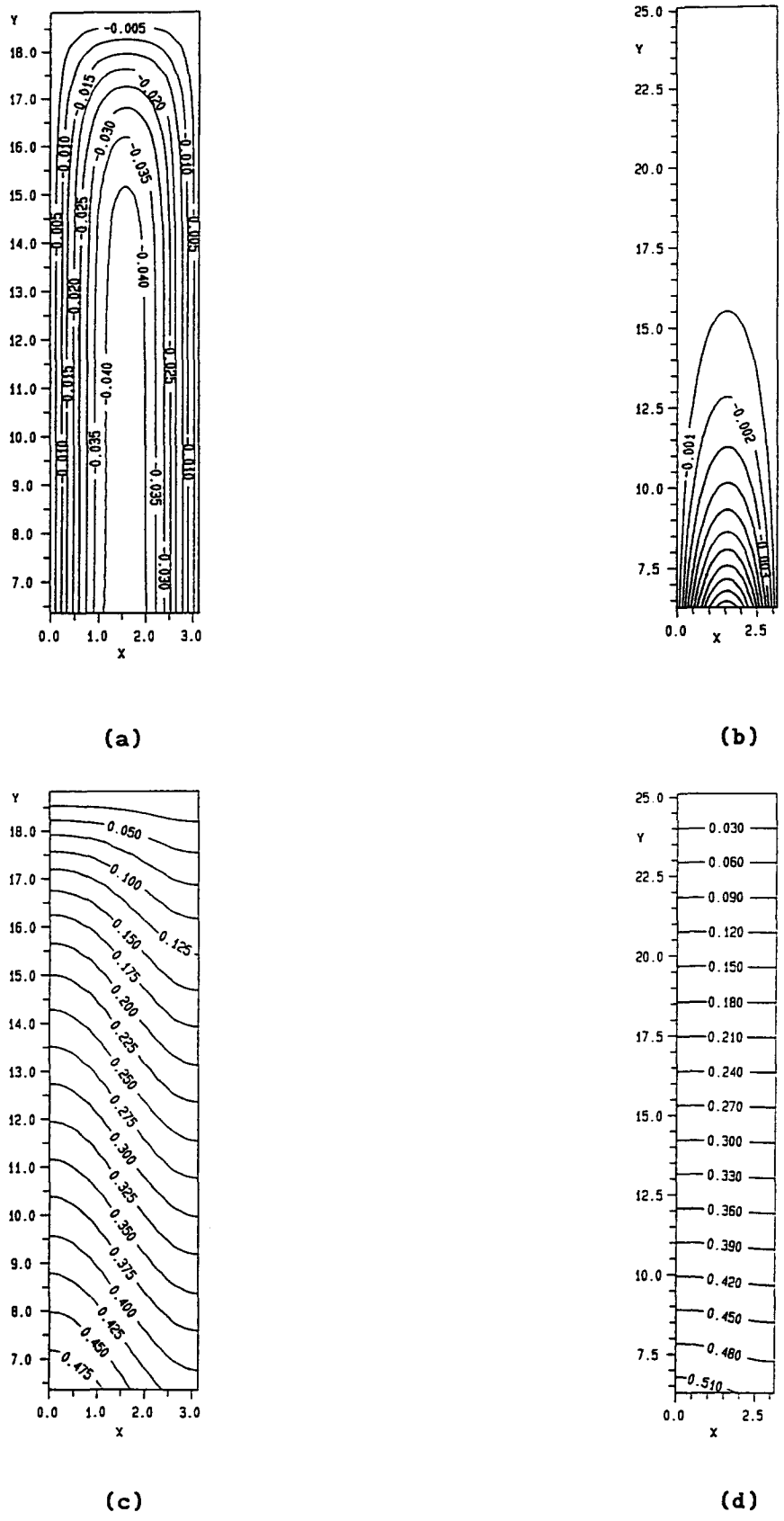

Fig. 3. Streamlines (a), (b) and isotherms (c), (d) for $Ra = 100/\pi$ plotted in the region $\{0 \leqslant x \leqslant \pi, 2\pi \leqslant y \leqslant d\}$ using the fixed temperature boundary condition (12) at $y = d = 6\pi$ and 8π, respectively.

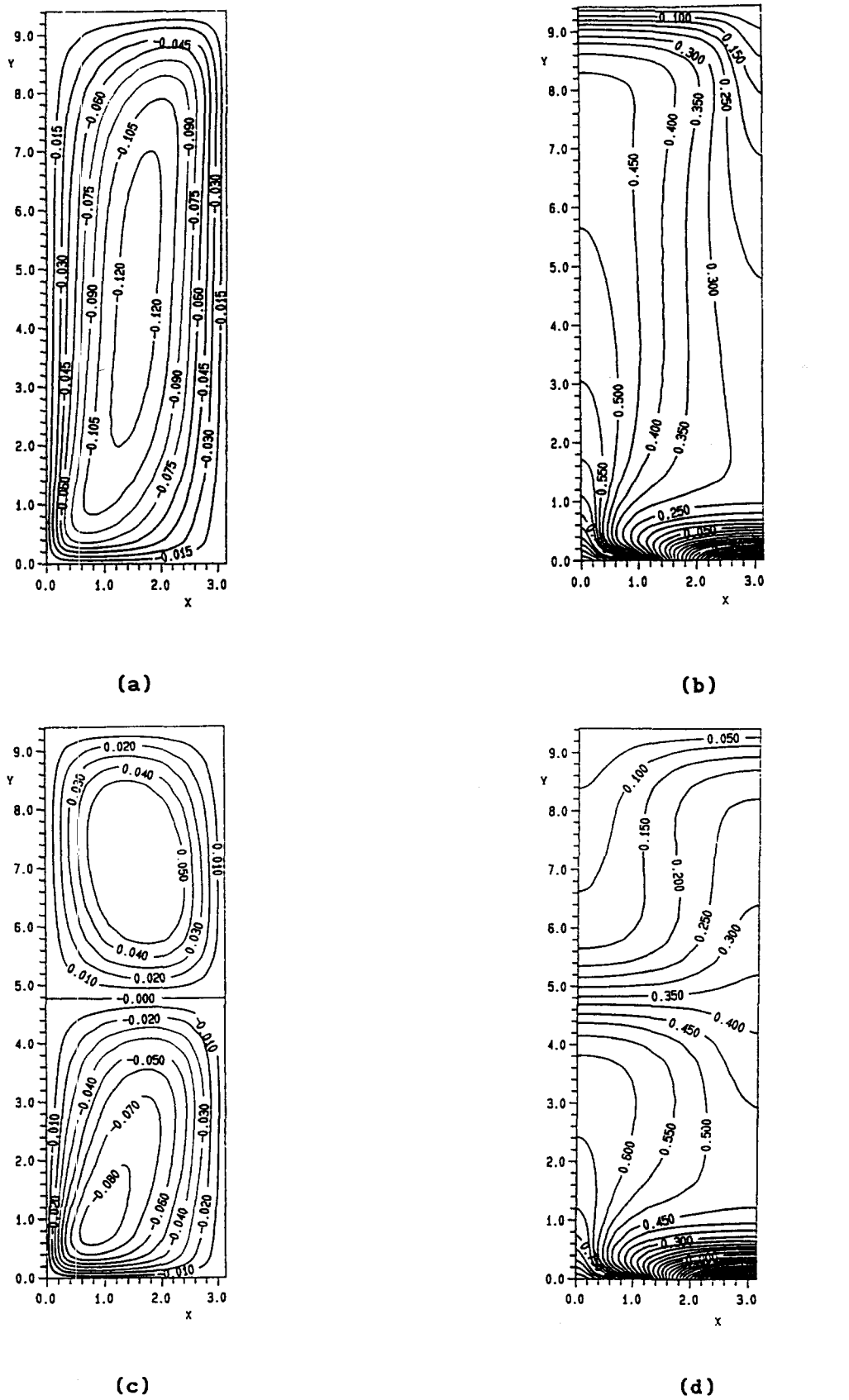

Fig. 4. Streamlines (a), (c) and isotherms (b), (d) of the unicellular and bicellular solutions, respectively, for $Ra = 200/\pi$ plotted in the domain D_a using the fixed temperature boundary condition (12) enforced at $y = d = 3\pi$.

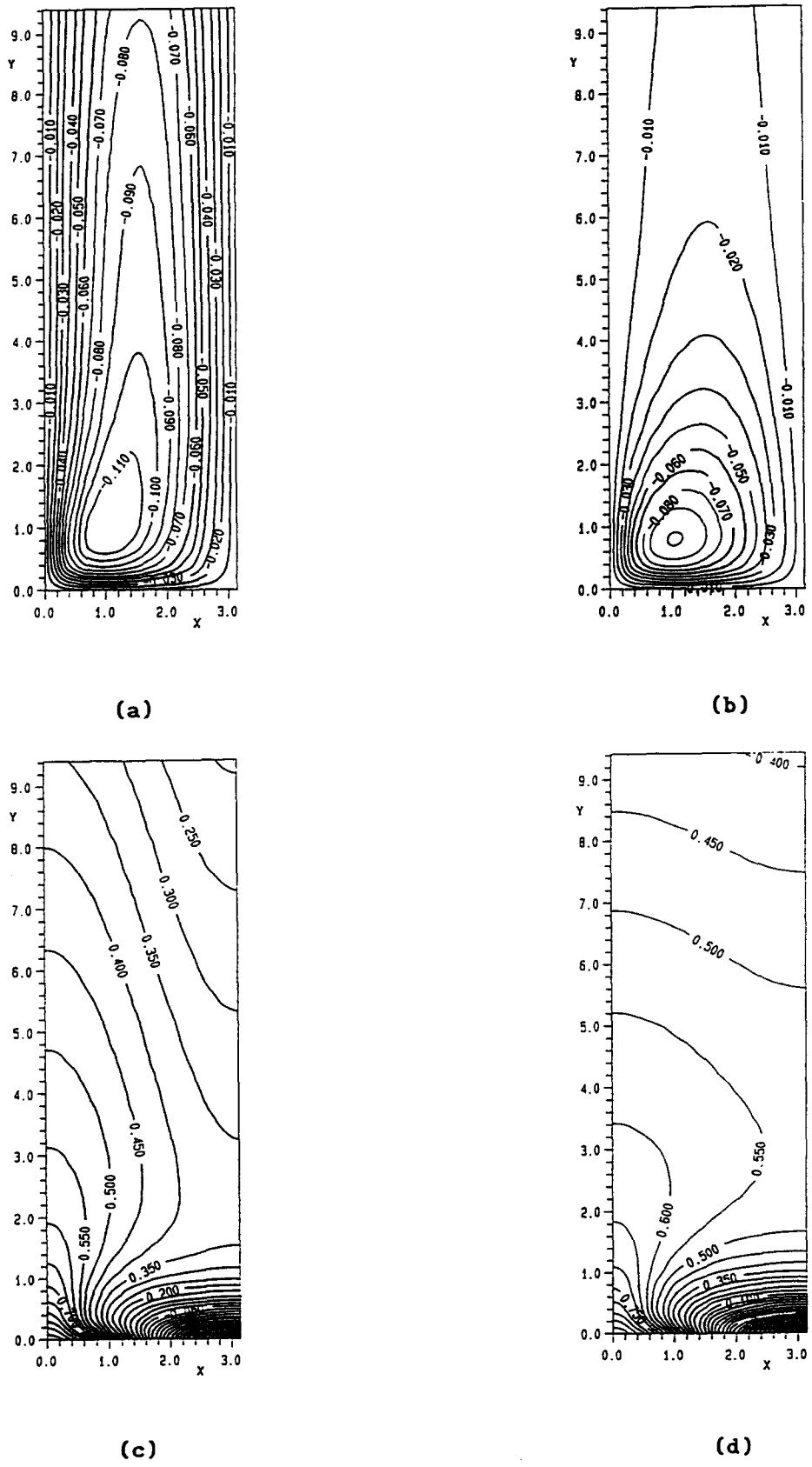

Fig. 5. Streamlines (a), (b) and isotherms (c), (d) for $Ra = 100/\pi$, $\varepsilon = 10^{-3}$ and 10^{-9}, respectively, plotted in the region $\{0 \leqslant x \leqslant \pi, 0 \leqslant y \leqslant 3\pi\}$ using the fixed temperature boundary condition (12) at $y = d = 7\pi$.

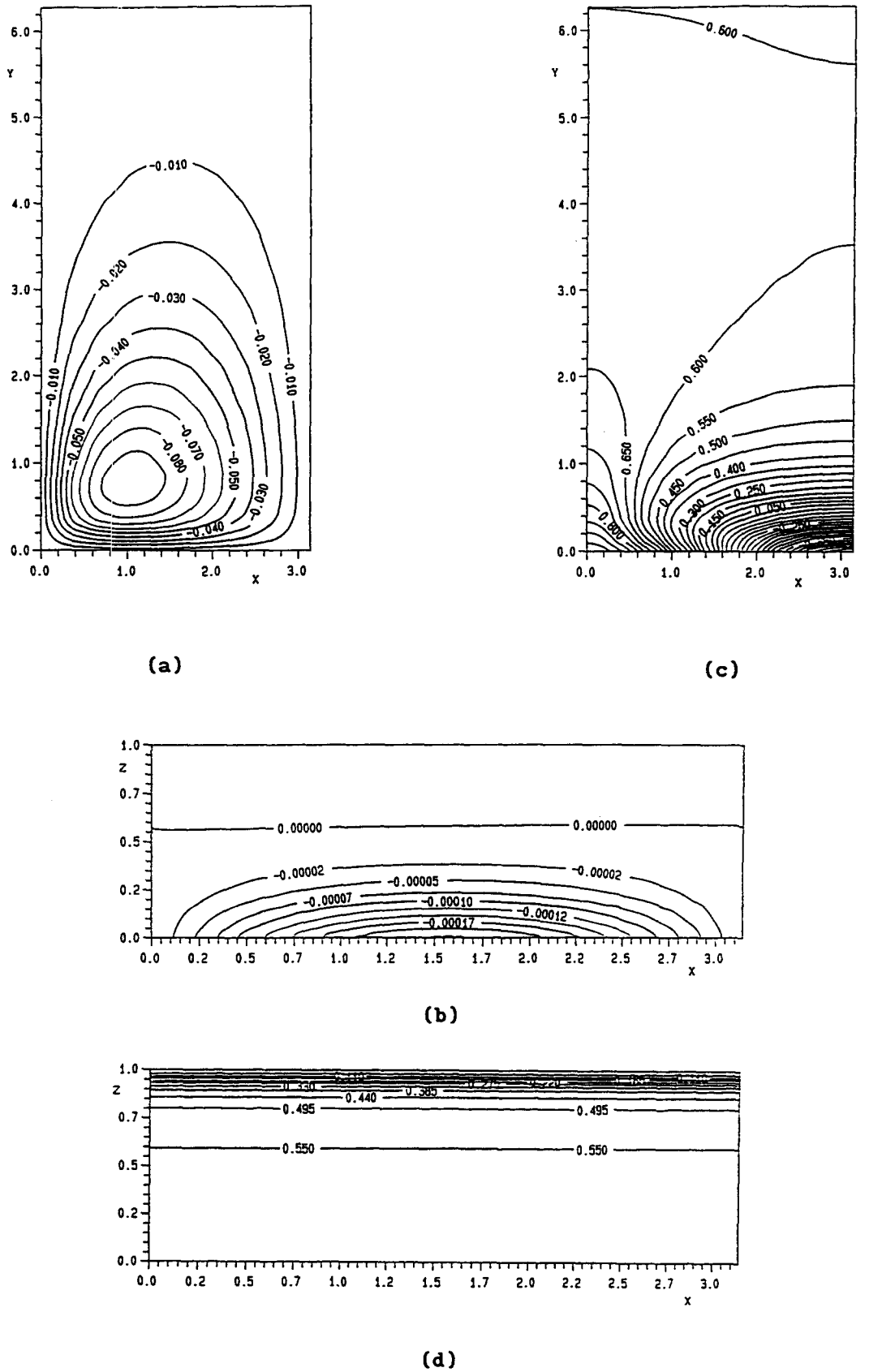

Fig. 6. Streamlines (a), (b) and isotherms (c), (d) plotted in the domains $\{0 \leqslant x \leqslant \pi, 0 \leqslant y \leqslant 2\pi\}$ and D_c, respectively, for $Ra = 100/\pi$ and 100 000 iterations using the fixed temperature boundary condition (12) at infinity with $d = 3\pi$.

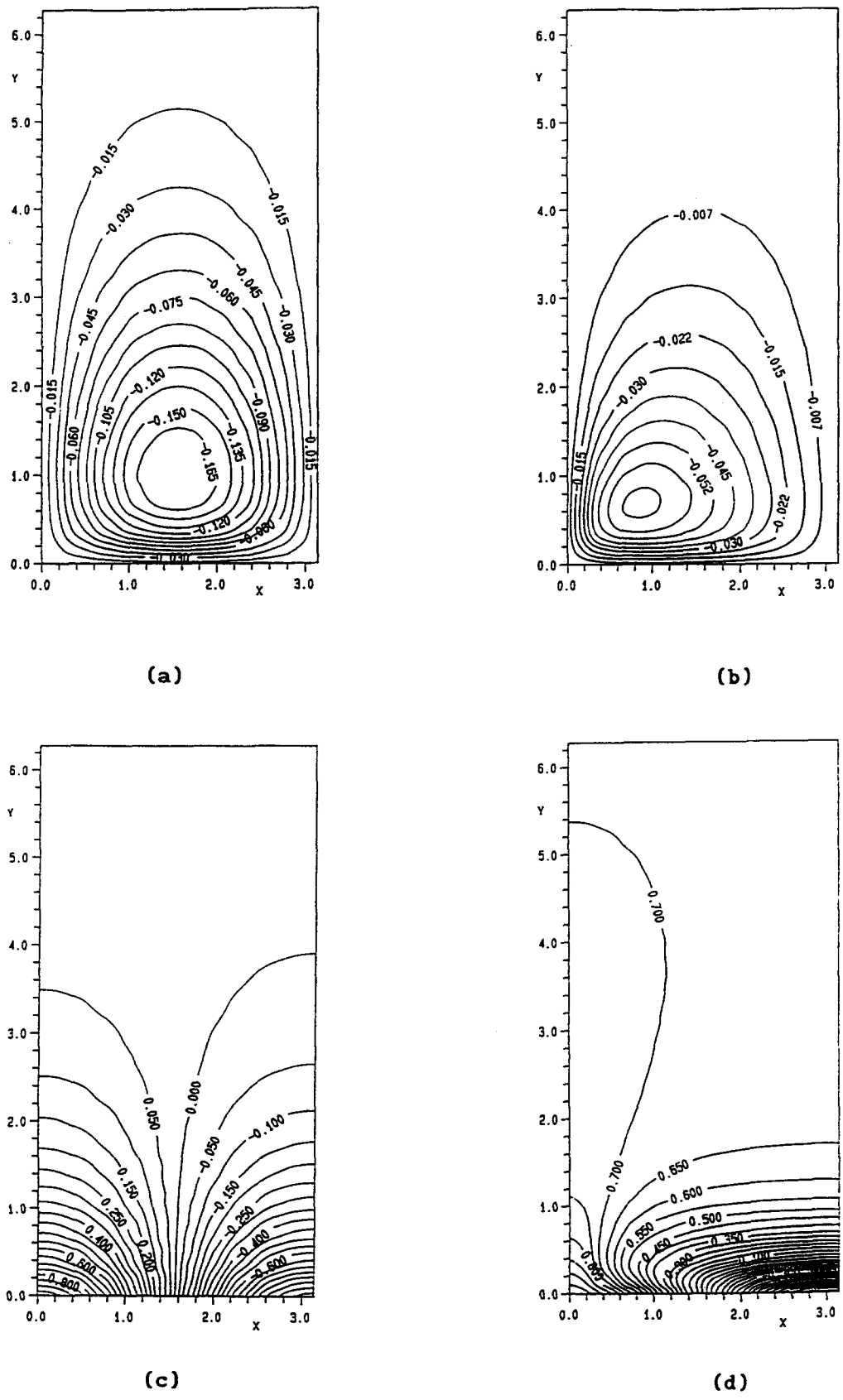

Fig. 7. Streamlines (a), (b) and isotherms (c), (d) for $Ra = 1/\pi$ and $200/\pi$, respectively, plotted in the region $\{0 \leqslant x \leqslant \pi, 0 \leqslant y \leqslant 2\pi\}$ using the adiabatic boundary condition (13) at infinity with $d = 4\pi$.

Table 1. Comparison of the analytical (A) and numerical (N) flow characteristics for $Ra = 1/\pi$ and different values of d when the fixed temperature boundary condition (12) is enforced at $y = d$

d		4π	5π	6π	7π
$\bar{u}$	A	−1.0000	−1.0000	−1.0000	−1.0000
	N	−0.9985	−0.9985	−0.9985	−0.9985
$\overline{Nu}$	A	1.0025	1.0020	1.0017	1.0014
	N	1.0024	1.0019	1.0016	1.0013
$\bar{Q}$	A	−0.0050	−0.0040	−0.0033	−0.0028
	N	−0.0043	−0.0033	−0.0026	−0.0021
$T(0, d-\pi)$	A	0.0050	0.0040	0.0033	0.0028
	N	0.0051	0.0040	0.0033	0.0028
$T(\pi, d-\pi)$	A	0.0049	0.0040	0.0033	0.0028
	N	0.0049	0.0040	0.0033	0.0028

locations is trapped near the wall, the temperature of one cell resembles more closely some hot temperature rather than the constant temperature considered at large distances from the plate.

For small values of Ra we found good agreement between the analytical and numerical solutions in the situation in which the boundary condition (12) is enforced at a finite distance $y = d$ from the wall. This agreement is presented in Table 1, which contains the values of the mean velocity along the plate $\bar{u}$, the mean Nusselt number $\overline{Nu}$ and the average heat flux at the plate $\bar{Q}$ for $Ra = 1/\pi$ and $d = 4\pi$, 5π, 6π and 7π. The values of the temperature at $x = 0$ and π for $y = d-\pi$, i.e. at the location where the zero temperature boundary condition was previously enforced, have also been included in this table. We observe that the temperature at $x = 0$ and π has small positive values, which are almost equal. However, the agreement between the analytical and numerical solutions as the distance d increases indicates that the slight dependence of the numerical solution on the parameter d is not an error introduced by enforcing the boundary condition (12) at $y = d$ rather than at infinity, since in the limit $d \to \infty$ the analytical temperature solution gives a non-zero constant temperature, namely $T_1 \to 1/16$. The streamline and isotherm patterns for $Ra = 1/\pi$ and $d = 7\pi$ are plotted in Figs. 1(a) and (b), respectively, and we found that at very small values of Ra the streamline and isotherm patterns obtained for different values of $d \leqslant 4\pi$ are almost indistinguishable. However, as Ra increases, the numerical solution becomes more dependent on the parameter d, see Table 2 for $Ra = 100/\pi$. The effect of increasing the value of d on the streamline and isotherm patterns is best illustrated in Figs. 2 and 3 for $Ra = 100/\pi$ and $d = 6\pi$ and 8π. It is seen that as d increases the flow changes from a situation in which a cell occupies the entire domain D_a into a situation in which the cell occupies only a part of the region of the domain D_a, which is of a height $H < d$, see Fig. 3. For $Ra = 100/\pi$ the critical distance $d = d_c$, up to which the flow occupies the entire domain D_a, is in the range $6\pi < d_c < 7\pi$. Numerical results obtained for different values of Ra showed that d_c increases with increasing Ra. As d increases above d_c, the velocity along the plate and the height H of the cell decreases according to a very small horizontal temperature gradient for $y > H$. However, the temperature calculated at the location $y = d-\pi$ clearly shows that the hot temperature is convected to larger and larger distances from the plate as d increases.

When the Rayleigh number is increased above a value of about $150/\pi$, we found range of values of d in the range $3\pi \leqslant d \leqslant 8\pi$ for which two different numerical solutions exist. Merkin and Zhang [5] also obtained two finite-difference solutions, i.e. a unicellular and a bicellular solution, for the free convection in a horizontal porous channel with the bottom wall being heated, by considering two different initial guesses for the Successive Over Relaxation method. However, for the problem under consideration, the two numerical solutions were obtained by numbering the grid points in the iterative method in two ways in the x direction. We found that the flow is unicellular when the grid points are numbered from the cold to the hot locations on the plate, see Figs. 4(a)

Table 2. Variation of the flow characteristics with d for $Ra = 100/\pi$ using the fixed temperature boundary condition (12) imposed at $y = d$

d	5π	6π	7π	8π
$\bar{u}$	−0.7396	−0.7262	−0.7188	−0.7171
$\overline{Nu}$	2.1725	2.0709	2.0151	2.0028
$\bar{Q}$	−0.3251	−0.1595	−0.0712	−0.0520
$T(0, d-\pi)$	0.2843	0.1989	0.1104	0.0864
$T(\pi, d-\pi)$	0.1354	0.1159	0.1001	0.0861

Table 3. The mean flow characteristics for the unicellular (U) and bicellular (B) flow for $Ra = 150/\pi$ and $200/\pi$ using the fixed temperature boundary condition (12) enforced at $y = d = 3\pi$

Ra		$\bar{u}$	$\overline{Nu}$	$\bar{Q}$
$\frac{150}{\pi}$	U	−0.718	3.103	−1.297
	B	−0.676	2.622	−0.490
$\frac{200}{\pi}$	U	−0.671	3.587	−1.636
	B	−0.631	2.998	−0.646

and (b) which contain the streamlines and isotherms, respectively, for $Ra = 200/\pi$ and $d = 3\pi$, whereas in the reverse situation when they are numbered from the hot to the cold locations on the plate the flow consists of two counter rotating cells situated one above another, see Figs. 4(c) and (d) in which the streamlines and isotherms, respectively, are plotted for $Ra = 200/\pi$ and $d = 3\pi$. Table 3 presents the values of the mean velocity, the mean Nusselt number and the average heat flux at the plate for $Ra = 150/\pi$ and $200/\pi$ and $d = 3\pi$ and shows that for the unicellular solution the velocity along the plate is greater and the heat transfer near the plate intensified than for the bicellular solution. For any other values of Ra and d the numerical solution does not depend on the numbering of the grid points in the iterative method, and the solution is unicellular.

As we have mentioned before, Poulikakos and Bejan [6] have presented numerical solutions and a scale analysis for this problem. However, they obtained numerical solutions using only the boundary condition (12) enforced at a finite distance d from the plate and a rigorous study of the dependence of the solution on the parameter d and on the convergence parameter ε given in equations (59) and (60) was not considered. In order to show the critical dependence of the numerical results on the value of ε, the streamline and isotherm patterns are given in Fig. 5 for $Ra = 100/\pi$, $d = 7\pi$ and $\varepsilon = 10^{-3}$ and 10^{-9}. It should be noted that for $\varepsilon = 10^{-3}$ we have obtained streamlines and isotherms of a similar form to those reported in [6], see Fig. 3 from [6], and the accompanying Fig. 5. However, these flow patterns change significantly as ε decreases to a value of 10^{-9}. It has been found that any further decrease in the value of ε produces results which are graphically indistinguishable from those obtained with $\varepsilon = 10^{-9}$. Therefore, it is likely that if the iterative method of Poulikakos and Bejan [6] is extended until the results were more accurate then their results would agree more closely with our convergent results as shown in Figs. 1–5.

Further, we have performed numerical calculations when the boundary condition (12) is enforced at infinity. Thus, equations (4) and (5) were solved in the domain D_a and equations (51) and (52) were solved in the domain D_c. In this case we were able to investigate the numerical solution at very large distances from the plate provided that the mesh points near $z = 1$ in the domain D_c are transformed in the domain D_b into points situated at a distance from the plate greater than $y = 280$. However, we found that the iterative method for this situation could not be considered to have converged, the values of $\Delta\psi$ and ΔT being $\mathbf{0}(10^{-6})$ after $\mathbf{0}(10^5)$ iterations. The streamlines and isotherms obtained in the domains D_a and D_c are plotted in Fig. 6 for $Ra = 100/\pi$, $d = 3\pi$ and 100 000 iterations. The difficulty in obtaining convergent results occurs near $z = 1$, i.e. at very large values of y, and the numerical results obtained show that as the number of iterations increases the solution appears to settle to an almost convergent solution in the domain D_a. Further, the mean velocity along the plate and the mean Nusselt number also appear to be converging as the number of iterations increases, see Table 4. On the other hand, the temperature appears to approach a constant value for values of z in the range $0 \leqslant z \leqslant 1/2$. As the value of z increases above about one half, the temperature decreases rapidly to zero near $z = 1$. The effect of increasing the number of iterations is that the constant temperature solution in the domain D_c expands to larger values of z and the temperature falls more rapidly near $z = 1$, i.e. the solution appears to be tending towards the one with a boundary-layer at infinity.

According to the analytical solution for small values of Ra, we now consider the case of the boundary condition (13), i.e. when $\partial T/\partial y = 0$ is enforced at $y = d$. Numerical solutions were obtained for various values of d in order to investigate the dependence of this solution on the values of d. It was obtained that for the range of values of Ra considered, the value of $d = 4\pi$ appears to be sufficiently large for the solution to be independent of the choice of d. When the boundary condition (13) is enforced at infinity and $d = 4\pi$,

Table 4. The mean velocity, the mean Nusselt number and the temperature at the locations $x = 0$ and π and $y = 3\pi$ for $Ra = 100/\pi$ obtained after different numbers of iterations using the fixed temperature boundary condition (12) at infinity and $d = 3\pi$

Iterations	ΔT	$\bar{u}$	$\overline{Nu}$	$T(0, 3\pi)$	$T(\pi, 3\pi)$
5000	1.2×10^{-5}	−0.7157	1.9919	0.4702	0.4674
20 000	7.3×10^{-6}	−0.7128	1.9708	0.5390	0.5384
50 000	3.0×10^{-6}	−0.7118	1.9629	0.5682	0.5680
100 000	1.5×10^{-6}	−0.7112	1.9589	0.5834	0.5832

Table 5. Comparison between the analytical (A) and numerical (N) solutions for different values of Ra using the adiabatic boundary condition (13) enforced at infinity

Ra		A	N
$\frac{1}{\pi}$	$\bar{u}$	−0.9999	−0.9984
	$\overline{Nu}$	1.0003	1.0000
	$\bar{Q}$	0	0.0007
	$T_{\inf}$	0.0199	0.0199
$\frac{5}{\pi}$	$\bar{u}$	−0.9979	−0.9930
	$\overline{Nu}$	1.0087	1.0124
	$\bar{Q}$	0	0.0033
	$T_{\inf}$	0.0989	0.0975
$\frac{10}{\pi}$	$\bar{u}$	−0.9914	−0.9781
	$\overline{Nu}$	1.0348	1.0479
	$\bar{Q}$	0	0.0065
	$T_{\inf}$	0.1943	0.1848

the numerical solution in the domain D_a is identical to within four decimal places to the solution obtained by enforcing the boundary condition (13) at $y = 4\pi$. In the domain D_c it is also obtained that the streamfunction is zero and the temperature is a constant (which depends on the Rayleigh number) to within four decimal places.

Table 5 shows the values of $\bar{u}$, $\overline{Nu}$, $\bar{Q}$ and $T_{\inf}$ calculated both analytically and numerically for $Ra = 1/\pi$, $5/\pi$ and $10/\pi$. It is found that for small values of Ra, e.g. $Ra = 1/\pi$, there is good agreement between these solutions. However, they become less consistent as Ra increases since the terms in the analytical solution which are $\mathbf{0}(Ra^3)$ cannot be neglected. In order to check that the numerical solution is physically consistent, we examine the values of $\bar{Q}$ from Table 5. As no heat is being taken out of the system as $y \to \infty$ and at $x = 0$ and π, then there should be no heat being put into the system at $y = 0$, i.e. $\bar{Q} \equiv 0$, which is in agreement with the results presented in Table 5. It is also obtained that the magnitude of $\bar{Q}$ is always less than 2% of the mean Nusselt number for all of the values of Ra considered.

The streamline and isotherm patterns for values of $Ra = 1/\pi$ and $200/\pi$ are shown in Fig. 7 using the boundary condition (13) at infinity. It is seen that the flow consists of a row of counter rotating cells situated near the wall whose heights slightly decrease as Ra increases, see Figs. 7(a) and (b). However, an important feature of this problem is the temperature asymmetry of one cell, see Figs. 7(c) and (d), which is due to the fact that the fluid in contact with the cold region is trapped near the wall. Table 6 presents the values of the Nusselt number, the mean velocity along the plate and the temperature at infinity, for $Ra = 40/\pi$, $60/\pi$, $80/\pi$, $100/\pi$, $120/\pi$, $160/\pi$ and $200/\pi$. It is observed that, as the Rayleigh number increases, the ability of one cell to transfer heat into and out of the porous media increases despite the decrease in the velocity along the plate.

Finally, at large values of the Rayleigh number the boundary-layer scalings suggest that the mean velocity along the plate and the mean Nusselt number should be scaled as

$$\tilde{u} = \bar{u}Ra^{1/3} \quad \tilde{Nu} = \overline{Nu}/Ra^{1/3} \tag{61}$$

where $\sim$ denotes the boundary-layer approximation. The values of $\tilde{u}$ and $\tilde{Nu}$ are presented in Table 6 for $Ra = 40/\pi$, $60/\pi$, $80/\pi$, $100/\pi$, $120/\pi$, $160/\pi$ and $200/\pi$ and the results indicate that the scaling laws are obeyed by the numerical calculations. It should be noted that the velocity along the plate decreases as the heat transfer processes intensifies and this is confirmed by the scaling laws.

6. CONCLUSIONS

In this study we have examined the steady free convection fluid flow through a semi-infinite porous media due to a heated and cooled horizontal surface, by considering two situations, namely when a given temperature T_∞ or a zero heat flux is enforced at infinity. We could not obtain analytical solutions for small values of Ra when an arbitrary constant temperature T_∞ is enforced at infinity but only when there is a zero heat flux boundary condition. However, this solution is approached by the solution obtained enforcing the temperature T_∞ at a finite distance from the plate $y = d$, as $d \to \infty$. Therefore, it is concluded that the appropriate boundary condition for the present problem is that of no heat transfer at an infinite distance from the plate. Numerically, we were unable to obtain a convergent solution when the temperature T_∞ is enforced at infinity, but only when it is enforced at $y = d$ and this solution is dependent on d. The analytical and numerical results obtained enforcing zero heat flux at infinity are found to be in very good agreement for small Ra, and showed that near the

Table 6. Values of the mean and boundary-layer flow characteristics for different values of Ra using the adiabatic boundary condition (13) imposed at infinity

Ra	$40/\pi$	$80/\pi$	$120/\pi$	$160/\pi$	$200/\pi$
$\bar{u}$	−0.8551	−0.7470	−0.680	−0.632	−0.596
$\tilde{u}$	−1.9967	−2.1977	−2.290	−2.343	−2.380
$\overline{Nu}$	1.3952	1.7904	2.090	2.332	2.537
$\tilde{Nu}$	0.5975	0.6086	0.621	0.629	0.635
$T_{\inf}$	0.4639	0.5878	0.644	0.677	0.699

heated and cooled horizontal surface the natural circulation consists of a row of counter rotating cells whose heights decrease as the Rayleigh number increases. The ability of one cell to transfer heat into and out of the porous media increases as Ra increases, despite the decrease in the velocity along the plate.

REFERENCES

1. D. A. Nield and A. Bejan, *Convection in Porous Media.* Springer, New York (1992).
2. P. Cheng and W. J. Minkowycz, Free convection about a vertical flat plate embedded in a porous medium with application to heat transfer from a dike, *J. Geophys. Res.* **82,** 2040–2044 (1977).
3. P. Cheng and I-Dee Chang, Buoyancy induced flows in a saturated porous medium adjacent to impermeable horizontal surfaces, *Int. J. Heat Mass Transfer* **19,** 1267–1272 (1976).
4. S. Kimura, A. Bejan and I. Pop, Natural convection near a cold plate facing upward in a porous medium, *J. Heat Transfer* **107,** 819–825 (1985).
5. J. H. Merkin and G. Zhang, Free convection in a horizontal porous layer with a partly heated or cooled wall, *J. Engng Math.* **24,** 125–149 (1990).
6. D. Poulikakos and A. Bejan, Penetrative convection in porous medium bounded by a horizontal wall with hot and cold spots, *Int. J. Heat Mass Transfer* **27,** 1749–1757 (1984).
7. D. Poulikakos and A. Bejan, Natural convection in a porous layer heated and cooled along one vertical side, *Int. J. Heat Mass Transfer* **27,** 1879–1891 (1984).
8. B. Zeldin and F. W. Schmidt, Developing flow with combined forced-free convection in an isothermal vertical tube, *J. Heat Transfer* **94,** 211–223 (1972).